CHARGE DISTRIBUTION AND ELECTROLUMINESCENCE IN XLPE UNDER DC FIELD

G. Teyssedre and C. Laurent
Université Paul Sabatier, Laboratoire de Génie Electrique, France

G. C. Montanari and F. Palmieri
University of Bologna, Department of Electrical Engineering, Italy

A. See, L.A. Dissado, and J.C. Fothergill
University of Leicester, Department of Engineering, England

ABSTRACT

The intent of this paper is to cross-correlate the information obtained by space charge distribution analysis and electroluminescence (EL) detection in cross-linked polyethylene samples submitted to DC fields, with the objective to make a link between space charge phenomena and energy release as revealed by detection of visible photons. Space charge measurements carried out at different field levels by the pulsed electro-acoustic method show the presence of a low-field threshold, close to 15 to 20 kV/mm, above which space charge begins to accumulate considerably in the insulation. Charges are seen to cross the insulation thickness through a packet-like behavior at higher fields, starting at about 60 to 70 kV/mm. EL measurements show the existence of two distinct thresholds, one related to a continuous excitation of EL under voltage, the other being transient EL detected upon specimen short-circuit. The former occurs at values of field corresponding to charge packet formation and the latter to the onset of space charge accumulation. The correspondence between pertinent values of the electric field obtained through space charge and EL analyses provides a support to the existence of degradation thresholds in insulating materials. Particular emphasis is given on the relationship between charge packet formation and propagation, and electroluminescence. Although the two phenomena are observed in the same field range, it is found that the onset of continuous EL follows the formation at the electrodes of positive and negative space charge regions that extend into the bulk prior to the propagation of charge packets. Charge recombination appears to be the excitation process of EL since oppositely charged domains meet in the material bulk. To gain an insight into specific light excitation process associated with charge packet propagation, electroluminescence has been recorded for several hours under fields at which charge packet dynamics were evidenced. It is shown that current and luminescence oscillations are detected during charge packet propagation, and that they are in phase. Mechanisms underlying EL and charge packets are further considered on the basis of these results.

1. INTRODUCTION

Space charge in polyethylene, especially in cross-linked materials (XLPE), has been the subject of many reports during the last decades [**1, 2, 3**]. Indeed, this material is widely used as insulation for power cable and there is an increasing need to understand the behavior of space charge, which is a limiting factor for the use of XLPE under DC stress. Space charge might also play a role in AC ageing and more and more studies aim at understanding space charge phenomenology in AC situation [**4, 5, 6, 7**]. On the other hand, ageing indicators have to be identified and diagnostic methods must be developed to evaluate the state of ageing of the insulation working under AC. Pertinent values linked to the ageing degree of the material could be used as input parameters for prognostic models. However, the ageing indicators are still largely to be unraveled. These are the main objectives of a EEC founded project entitled "Ageing and Reliability Testing and Monitoring of Power Cables: Diagnosis for Insulation System" (ARTEMIS) under which this study has been performed.

This paper focuses on the DC behavior of XLPE insulation as this is thought to be useful to diagnose the ageing of insulation working under AC stress.

Different reports describing the internal distribution of space charge in XLPE materials under DC field have been published recently. Experiments carried out either on lab specimens [**1, 9**] or on model cables [**8**] allowed to follow the charge distribution up to breakdown field. A technique well suited to follow the charge dynamics in dielectrics is the Pulsed Electro-Acoustic method (PEA). This technique was used in this study to investigate the charge distribution in XLPE peelings of ≈150 μm in thickness taken from high voltage cables. Electroluminescence will be defined in our context as the light emitted by the material under electric stress, or following the application of the stress. Its occurrence needs the mediation of excited molecular states, which are metastable states, and may provide a route to chemical decomposition. The onset of EL might therefore define an onset for ageing [**10, 11**]. It is thought that EL detection can give access to critical values of the applied stress in terms of stress magnitude and stress dynamics above which ageing mechanisms can be triggered. The theory of electroluminescence in large band gap materials predicts different excitation mechanisms depending on the type and distribution of carriers inside the dielectric. Light can be emitted upon inelastic interactions between mobile carriers (so-called hot carriers with kinetic energy >> thermal energy) and molecules constituting the dielectric. Although structural and chemical changes induced by hot electrons have often been evoked in electrical ageing [**12**], a clear evidence of their existence in polymeric insulation has never directly been given. The occurrence of hot carriers in model compounds of polyethylene material has been shown to be strictly limited to fields larger than about 60 % of the impact-ionization threshold field [**13**]. Hot electrons might be produced without space charge mediation if the applied field is in the pre-breakdown range (see Figure 1a). They could also be produced in the field-enhanced region in the case of a unipolar injected space charge (see Figure 1b). The other excitation mechanism of EL is encountered when bipolar injection and transport occurs (see

Figure 1c). In that case EL can be produced in the region where the recombination cross-section is the highest. To date, there are few reports on the detection of EL in PE under DC stress. One paper reports on a very faint light emission [**14**] but there were no correlative measurements and therefore no basis to discuss the excitation mechanisms. The objective of this paper is to perform a combined analysis of space charge profiles and electroluminescence regimes in order to discuss the nature of the EL excitation mechanisms, and to compare the onset of ageing derived from literature work and models with those derived from EL detection.

It has recently been shown that space charge accumulation in polyethylene can be described using a threshold field below which the amount of stored charge is very little (sensitivity limit ≈ 0.1 $C.m^{-3}$) and has a small dependence on field, and above which space charge accumulation is strongly increased [**15**]. This was achieved by recording the charge profiles on a sample submitted to increasing levels of DC field for some selected time (order of hours), and by quantifying the net charge stored in the dielectric at each field level for the selected time. The order of magnitude of this threshold field is in the range 10-20 kV/mm depending on materials. It was proposed that this field value might be associated with an onset for ageing. A theoretical basis of the ageing mechanism has been developed accordingly [**16**]. In the low field range, far from breakdown field, the occurrence of EL would inherently be related to the presence of space charge. The detection of EL in this field range would therefore constitute an evidence for space charge accumulation. Correlation between the onsets for space charge accumulation and EL occurrence might provide further support to the existence of an ageing threshold. Previous studies gave indications in that direction [**17**]. A detailed analysis of this topic will be presented here.

The time-dependence of charge profiles has been reported not only in short-circuit (volt-off) conditions but also during voltage application (volt-on). It has been shown that above a material dependent field value of the order of 70-100 kV/mm [**1**], the space charge can acquire a dynamic character as compared to the situation under lower field. The most striking fact is the organization of the space charge under the form of charge packets that cross the insulation [**1, 8, 17, 18, 19**]. They appear as apparent motion of charge particles (being either positive [**8**] or negative [**19**] depending on materials [**19**], LDPE, XLPE, doped or undoped) that are liable to cross the gap between the electrodes with apparent mobilities of the order of 10^{-15} $m^2V^{-1}s^{-1}$ [**18**]. The electric field is greatly enhanced in front of the packet, and is relaxed at the tail, according to the schematic drawing of Figure 2. Two different interpretations have been put forward. The charge packet is described either as a body of excess charge initiated by injection from the electrodes [**8, 18**], or as a propagating ionisation front [**1, 19, 20, 21**]. In the latter case field-induced ionisation of impurities contained in the material occurs in front of the propagating wave, which leads to the supply of carriers to the bulk. Depending on the difference between mobilities of positive and negative carriers, positive or negative packets can be detected. Models of a propagating ionisation front have been proposed in which different levels of traps were needed to fit the results of experiment [**21**]. Whatever the origin of the charge packet, one

important feature of the models is that they involve charge recombination. This will occur either at the tail of the propagating packet if the phenomenon is due to the propagation of an ionisation front (see Figure 2) or during the propagation if the packet is a body of excess charge. As the recombination region is potentially a luminescence one it is of interest to record the EL in this regime. This topic will also be addressed.

The paper is organized along the following lines. In section 2, we give the experimental details concerning the samples and the detection methods. The results are discussed in section 3. The EL vs. field characteristic determined from a progressive DC stress test is reported in § 3-1. It is shown that the EL is continuously excited during the application of the DC stress provided the applied field exceeds a given value, called onset field for continuous EL excitation and referenced as E_{EL} in the following. In the range of field below E_{EL}, luminescence can be excited during the transients at voltage application or sample grounding provided the polarization conditions were adequate. The mechanisms at play are discussed in § 3-2 on the basis of the space charge profiles. For fields higher than E_{EL}, it is shown that the space charge acquires a dynamic character as compared to the situation below E_{EL}. The excitation mechanisms of continuous EL are discussed in § 3-3. Finally, the relationship between EL and charge packet is discussed in § 3-4.

2. EXPERIMENTAL

2.1. XLPE samples

The specimens were obtained from films peeled from unaged cables produced using extra-clean materials and processes. Three reference cables (Cable A, B and C) were considered with the same formulation for the insulation and small differences in the extrusion process and semi-conductor composition. The insulation thickness was 14 mm and 27 mm and dicumyl peroxyde was used as the cross-linking agent. Peels that were investigated were taken at a distance from the inner semi-conductor comprised between 2 and 4 mm in order to minimize the influence of low molecular weight contaminants migrating from it. A complete description of the preparation steps is described elsewhere [**22**]. It involves the peeling itself that was done using a lathe equipped with a specially designed knife to get optimum surface smoothness, the selection of samples in rolls according to the selected distance from the inner semi-conductor, and a thermal treatment. A careful observation of the peels quality using Atomic Force Microscopy revealed that they have different surface roughness on both sides (r.m.s. roughness of 150 nm vs 350 nm), and different surface microstructure in a depth of the order of 5 to 10 μm [**22**]. These dimensions are small as compared to the thickness of the peeling which is, on average, 150 μm. A thermal treatment was carried out at 50 °C for 48 hours in order to expel most of the residues of the cross-linking process. The concentration of cross-linking by-products (cumyl alcohol, acetophenone, α-methylstyrene, cumene) measured after such treatment was below the

detection level of Fourier Transformed Infrared Spectroscopy and High Performance Liquid Chromatography [**22**].

2.2. Space charge and external current measurements

Space charge measurements were performed by the pulsed electro-acoustic technique at various DC-voltages varying from 1 to 150 kV/mm. Two different PEA systems were used, one of those allowing simultaneous measurement of the external current with a sensitivity of 10^{-14} A [**5**]. Measurements were performed in air or in controlled atmosphere (nitrogen) at room temperature. The sensitivity limit of the two systems is about 0.1 $C.m^{-3}$ and their spatial resolution of the order of 10 μm. The poling scheme usually consisted of a poling time (10000 s) and a depolarization time, when the specimen is short-circuited, lasting 2000 s. Longer term experiments in which poling and depolarization lasted for 48 hours were also performed, as well as experiments under progressive DC stress test with steps lasting for shorter time. The electrodes in contact with the films were either semiconducting carbon-filled polyethylene (high voltage electrode, anode) and aluminum (cathode) electrodes of the PEA system, or gold electrodes deposited by cold sputtering on both faces of the specimens. Further details on the sample preparation and the experimental protocol adopted for each class of experiment are given in paragraph 3.

2.3. Electroluminescence and external current measurements

Electroluminescence was detected with a photomultiplier (PM) with a flat spectral response in the wavelength domain extending from 300 nm to 800 nm, and working in photon counting mode. Cooling the PM at –30 °C provides a low background noise of the order of a few counts per second (cps) which is a characteristic of each photomultiplier. We have used two different cells equipped with two different PM, having a noise level of about 1 cps and 5 cps. Small variations of the noise around these values can be observed depending on the time the PM spent in total darkness before the experiment. The noise is determined at the beginning and the end of every experiment to check for any evolution during the time scale of the observation which might be a problem when dealing with a level of light of the same order of magnitude as the PM noise. Specimens were metallized on both surfaces with semi-transparent layers of gold deposited by cold sputtering (the electrode area was 20 cm^2) and sandwiched between two brass electrodes with polished surfaces. The use of a ring electrode with an outer diameter smaller than the metallization diameter allowed the emission coming from the central part of the sample to be detected. All the tests were undertaken under high vacuum ($< 10^{-4}$ Pa) in order to avoid discharges. The characteristics of the detection set-up have already been given in the literature [**23**]. EL was recorded during polarization and depolarization, at different field levels and for different times of application of the stress. The external current was measured simultaneously with a sensitivity of 10^{-14} A. Details of the protocol used in each experiment are given in section 3.

3. RESULTS AND DISCUSSION

3.1. Determination of the EL onset from a progressive DC stress test

The first step in the analysis was to investigate the EL vs field characteristic by using a progressive DC stress test. The voltage was increased in constant steps up to a maximum value, and then decreased with the same voltage steps. EL and external current were recorded at constant voltage both in the increasing and decreasing cycle. The waiting time at each step was short (300 s upon increase, 150 s upon decrease), so that one could not consider that the steady state value of the current was reached. EL and current values have been averaged over the time range t>50 s at each step. A counting dwell time of one second was adopted for these measurements.

Two voltage cycles were applied consecutively on the same sample :

-0/120/0 kV/mm, with steps of 4.0 kV/mm

-0/150/0 kV/mm, with steps of 5.3 kV/mm.

Figure 3a shows the EL level obtained during the two voltage cycles as a function of the DC field for XLPE B. There is a clear departure of the PM signal from the noise at about 60 kV/mm. The EL measured during the decreasing part of the voltage cycle is slightly lower than that obtained during the increasing part at the same field. Examples of the time evolution of the EL at different field levels are shown in Figure 3b**.** The EL is continuously excited during voltage application and appears reasonably stable during the time scale of the observation (300 s), although a time-decreasing intensity of the EL is seen for the highest fields. A threshold for continuous EL detection (labeled E_{EL} in the following) can be determined at 60-70 kV/mm as seen in Figure 4. Note that the EL does not depend on the rank of the voltage cycle, contrary to what is observed for the current. As previously pointed out, the current values cannot be considered as representative of the conduction regime due to the short recording time at each voltage step. Below ≈80 kV/mm there is a strong effect of previous polarization of the sample as denoted by the current values that are higher during the second cycle. Currents are roughly the same above ≈80 kV/mm, which shows that the processes taking place in this field range are less dependent on the initial charging of the material. It is noteworthy that this field value corresponds to a change in slope of the current-field plot. Moreover, it is clearly correlated with the EL onset. Further confirmation of the correspondance between EL onset and a change in the transport mechanism, pictured by a change in slope of the current-field characteristic, was provided by long term recording of the current. The current-field characteristic obtained on gold-metallized XLPE B after 24 hours of polarization at each voltage step is shown in Figure 5. In this case, the current values can be considered as representative of the conduction process. It appears clearly that 60 kV/mm corresponds to a change in the I-E characteristic in exact correlation with the EL onset.

This correspondence between the onset of EL and a change of slope in the current-field characteristic has already been observed in different insulating polymers [**23**]. It is a strong indication that the EL

onset is a true physical threshold (as opposed to a sensitivity-limited threshold) corresponding to the onset of the excitation mechanism that is reflected by the marked change in the current-field characteristic. Experiments performed on different samples have shown a good reproducibility of the EL and current versus field in the high field domain. EL onset and change in slope in the current-field plot have always been found in good correlation. As an example, Figure 6 shows data obtained by testing a sample taken from cable A.

The values of the EL onset obtained on the three kinds of XLPE are given in Table 1. The three materials behave in a similar way. On the basis of these observations, we decided to focus on space charge profiles below and above the EL onset.

3.2. Charge profiles and transient EL below the onset for continuous luminescence

3.2.1. Phenomenology

A polarization/depolarization protocol was used to investigate charge profiles and EL. The procedure consisted in a polarization time (10000s for charge profile analysis, 3600 s for EL detection) followed by a depolarization time (2000 s for charge profile analysis, 3600 s for EL detection) at a given field level. The field was increased in steps of 5 kV/mm, and the same experiment was repeated. Charge profiles were continuously recorded during the polarization and depolarization time as well as EL. For both EL and PEA experiments, the samples were connected to the high voltage lead (polarization) or to the ground (depolarization) by the use of a high voltage switch. Gold metallized samples were used in both kinds of experiment.

PEA measurements show that below a field of the order of 15-20 kV/mm the space charge density is at the sensitivity limit of the detection system, which is close to 0.1 $C.m^{-3}$. Above 20 kV/mm space charge accumulates significantly, although the dynamic of space charge built-up is slow as shown in Figure 7a. Charge profiles obtained at the end of the polarization time for different values of the field are shown in Figure 7b. Heterocharges are seen to accumulate near the electrodes.

In agreement with the progressive DC stress test, the EL was not detected neither during permanent application of the voltage nor during the depolarization period, but it was during the transients associated with voltage application and grounding. Care was taken as to avoid electromagnetic interference between the high voltage switch and the PM counting circuit. We also checked that there was no overshoot in the voltage waveform when the voltage was turned on and off. A typical EL transient observed at HV application is shown in Figure 8a. The EL decays in a matter of a few seconds to reach the PM noise level. The transient is much faster during grounding as shown in Figure 8b. Its analysis necessitates a shorter sampling time (10 ms here).

Although we did not carry out a detailed analysis of the influence of the protocol used to apply the stress, it was obvious from our tests that EL excitation was favored by fast variations of the voltage such as those obtained by using the high voltage switch.

3.2.2. Space charge and electroluminescence quantification

A quantitative evaluation of the field above which charge accumulates can be obtained by resorting to the calculation of Q_m, called the total stored charge density. This is defined as the integral of the absolute value of the charge profile (excluding the image charges on the electrodes) [**15**], at a given depolarization time, e.g. 10 s. Although this quantity is a rough evaluation of the net accumulated charge, it can be taken as an indication of the ability of the material to store space charge. The value of Q_m obtained for XLPE A is plotted as function of poling field in Figure 9a. From this plot, the threshold above which space charge begins to accumulate in the insulation can be easily determined, i.e. above 20 kV/mm (as compared to 15 kV/mm for XLPE P and H).

A systematic study of the field-dependence of the transient EL at voltage application has not been carried out. However, its occurrence has been evidenced from about 40 kV/mm on, i.e. in a field domain where space charge are seen to accumulate. The transient EL could be due to the process of charge injection that is likely to become effective at this field level. The injected carriers might either recombine some heterocharges near the injecting sites of the electrodes, or can be accelerated at the electrode/dielectric contact where the mean free path of carriers can be higher than in bulk. Both processes would be time dependent through the time dependence of the interfacial field that is controlled by the amount of injected carriers, i.e. by the space charge trapped in the vicinity of the electrode.

The field-dependence of the transient EL at short-circuit has been carefully investigated. The integrated EL counts recorded at the short-circuit (see Figure 8b) are reported as a function of the poling field in Figure 9b for XLPE A. Here again, a threshold below which the EL emission is lower than the measuring system sensitivity and above which the EL is steeply increasing in magnitude is clearly defined at 20 kV/mm. EL occurrence in this field range can only be explained by the presence of space charge. If no space charge were present in the material, there would be no possibility for EL excitation upon grounding. A first insight into a possible excitation mechanism could rely on the analysis of the charge profiles recorded at the time of the short-circuit. However, the corresponding profiles did not show any fast modification of the charge, which precludes any conclusions on EL excitation. It might be due to the fact that EL is excited by local reorganization of the space charge in regions that are far beyond the spatial resolution of the PEA system, or that it involves changes in time scale lower than the PEA integration time (a few seconds in our measurements). Such analysis would require a faster acquisition of the charge profiles, which is out of the scope of the present investigation. However, detection of EL in such conditions is not only the evidence of the accumulation of space charge in the material. It denotes that a rapid change in the applied field is able to trigger off energetic processes through internal space charge reorganization. The above-defined threshold can therefore be seen as a limit value of the field above which electrostatic energy from

space charge can be dissipated to the dielectric during fast voltage variations, thus contributing to the triggering of degradation processes.

The good correspondence between the threshold estimates obtained by space charge and EL techniques (see Figure 9) shows that they provide consistent information regarding the space charge formation phenomenon. It is clear from the charge profiles that 20 kV/mm defines a limit above which space charge accumulates considerably. EL detection strengthens the view that this limit is associated with a degradation threshold. It is noteworthy here that a similar correlation between onsets of space charge accumulation and occurrence of transient EL at short-circuit has been reported in a totally different insulating polymer (polyethylene naphthalate-PEN) by using a different method to analyze the space charge profile (Laser Induced Pressure Pulsed Method) [**24**]. Owing to the different electrical properties of XLPE and PEN, the threshold value was 75 kV/mm in the latter.

3.3. Charge profiles and EL above the onset for continuous luminescence excitation

3.3.1.Phenomenology

Charge patterns describing space charge evolution with time clearly exhibit different features than those below E_{EL}. The striking fact is the dynamic character of the space charge, with the formation of so-called charge packets. We have carefully investigated the spatio-temporal evolution of the charge detected at 60, 80, 130 and 150 kV/mm using the polarization/depolarization procedure described in § 2. Charge packets are not seen at 60 kV/mm, but they are at 80, 130 and 150 kV/mm. A detailed analysis of the time and spatial dependence of the space charge, during polarization and depolarization, is proposed in Figure 10 for the four different field levels, in the case of gold-metallized XLPE B.

Charge packets are not seen at 60 kV/mm (Figure 10a) during the time scale of the experiment. Homocharges are observed to build-up at both electrodes at the beginning of the experiment, although this is better seen at the cathode. From about 1500 s on, there is a progressive regression of the homocharge region with a change to heterocharge, clearly seen at the anode. Heterocharge accumulation is confirmed in volt-off condition where the detection of space charge near the electrodes is no more smeared out by the capacitive charge due to the applied voltage (see Figure 11).

It is clear that the field would drive any charge towards the electrode of the opposite sign during voltage application. Three possibilities can be envisaged as regard the origin of charges: they can be originally present in the material as ionic species, be generated by field-assisted dissociation of neutral species, or be injected from the contacts. Charge profiles taken at lower fields (see Figure 7) show also heterocharge accumulation, which could indicate the presence of ionic species. Heterocharge stabilization could be associated with the blocking nature of gold electrodes. There is, however, evidence of charge injection at 60 kV/mm, especially at the cathode where there is negative space charge that reaches a maximum at about 1500 s. The amount of negative charges is seen to decrease afterwards due to the compensation by positive heterocharges accumulating near the cathode (PEA, as

any other method of space charge detection, gives access to the net charge only). This behaviour would increase the cathode field relative to the situation that prevails at the beginning of the experiment, thereby enhancing electron injection. The effect of the negative charge injection seems to be balanced by the accumulation of positive charges that, overall, predominates at the cathode. The same process occurs in the vicinity of the anode where negative charges accumulate and dominate over positive charges injected from the contact. There are also very small changes in the middle of the sample where positive and negative charges partially compensate to give an overall response dominated by the positive carriers.

At 80 kV/mm (see Figure 10b), the same processes of charge injection and heterocharge accumulation are observed, although with an enhanced amplitude and dynamic leading to charge packet detection. Initially, negative charge injection dominates at the cathode and a front of negative charge penetrates into the bulk up to the anode region. The charge profile taken at 200 s (see Figure 12a) indicates a field amplification of 10% at the anode that triggers the formation of a positive charge packet. The front of positive charge propagates towards the cathode (figure 10b), thereby enhancing the cathode field (see Figure 12a-charge profile taken at 1100 s). On the whole, negative charges are prevailing in the middle and near the electrodes, although the profile taken in volt-off conditions (see Figure 11) gives evidence of heterocharges at both electrodes. This leads to field enhancement near cathode and anode, which should favor charge injection. The effect of heterocharge accumulation becomes more and more pronounced as a function of time. Heterocharges not only dominate over homocharges at the anode, but their effect is also marked in the vicinity of the cathode where the negative charges are progressively compensated by positive charges.

The same processes are observed at 130 kV/mm (see Figure 10c). The injection and drift of negative carriers from the cathode (see Figure 12b-profile at 700 s) strongly enhance the anode field (see Figure 12c-profile at 700 s), leading to the formation of a positive charge packet at the anode and its propagation towards the cathode. The charge profile at time 10000 s (see Figure 12b) induces an increasing cathode field (see Figure 12c), although the anode field is still the strongest due to the net negative charge left behind the propagating positive charge packet. Heterocharges are detected accordingly in volt-off conditions (Figure 11).

When increasing the field further (150 kV/mm, Figure 10d), the dynamic of the packet propagation is increased. Basically, the scenario appears to be qualitatively similar to the one described previously. Homocharge regions are formed by charge injection at both electrodes, and a packet is launched when a front of a given polarity induces a sufficient field enhancement at the opposite electrode. The propagating packet is usually positive for the material under consideration. It leaves a negatively charged region behind it. It is worth noting that a new positive packet is only launched when the previous positive packet has reached the cathode. This can be easily understood when looking at the charge and field profiles during launching, propagation and collapse of a positive packet, such as those shown in Figure 13. Upon launching, the field is a maximum at the front of the propagating packet and

is reduced at the anode. During propagation, the field increases drastically at the cathode and is progressively restored at the positive electrode where it reaches a maximum when the positive packet collapses, allowing a new packet to be launched. The anode field is thus modulated by the propagation of the positive charge packets. From the second packet on, the amplitude of the positive packets decrease in time during polarization as seen from Figure 10d. The accumulation of heterocharges near cathode and anode is seen in volt-on conditions, and their presence is confirmed in volt-off (Figure 11d). The fact that heterocharges are detected in volt-on condition gives the evidence that they are neither recombined totally by the injected charges, which would have left homocharge, nor compensated by them.

Overall, the charge distribution observed in these different experiments seems to be the result of charge injection at the electrodes, and drift of charges in the bulk which leads to the accumulation of heterocharges at both electrodes, the latter acting as blocking contacts. The important finding is that, although not always detected in volt-on condition due to the predominance of charges of opposite polarity, heterocharges are not totally recombined upon charge injection. They would therefore control the injection process during the entire experiment. The phenomenology of the charge packet formation and propagation is complex. In some of the long-term experiments the packets were not observed until a waiting period of some hours duration and subsequently die away over very long times. In all cases the launching of a positive packet is preceded by a field enhancement at the anode due to negative heterocharge. This appears to argue for an explanation in terms of a pulse of injected positive charge [1], and it can be noted that the applied field for the onset of packet formation in our experiments is in agreement with that of 70kV/mm noted in [1]. However, we have to point out that the amount of negative heterocharge left behind at the anode as the positive packet propagates towards the cathode is considerably greater than that measured prior to the launching of the packet. This latter fact indicates an origin for the packet in terms of the separation of pre-existing positive and negative charges into a mobile positive packet and residual negative charge trapped near the anode. The fact that the packet retains its integrity over some hours as it transits the sample against a permanent background of negative charge suggests that its nature cannot be simply that of a body of excess positive charge. Over a period of time the packets become weaker; possibly injection from the anode leads to recombination and is unable to completely replenish the positive charge reservoir required for packet formation, or trapping features are modified by the massive trap feeling associated with the first packets.

All models for packet formation [1,21] imply that recombination will occur, either as part of the mechanism of ionisation-recombination responsible for the packet itself, or through recombination of the excess charge in the packet with a background charge if it exists. We would therefore expect electroluminescence to be associated with the presence of charge packets in our samples. In fact our experiments indicate that at 60-70 kV/mm luminescence excitation becomes continuous, and thus appears to associate the EL excitation mechanism to the onset of charge packet formation as revealed

by the space charge measurements. However, the key question that has to be addressed is the exact relationship between EL and charge packet formation and propagation. It is indeed possible that packet formation is ancillary to a process that also leads to EL, such as the ability of opposite polarity charges to penetrate the insulation. In fact the charge profiles given in Figure 10 show that a homocharge situation prevails before the development of charge packets. Thus, charges of opposite signs drift in the insulation bulk. This would support an excitation of EL through recombination phenomena. Another observation leads to some doubt on the hypothesis that EL might be a consequence of charge packet. It is clear from the progressive DC stress test that there is no delay between voltage application and luminescence detection which seems in contradiction with Figure 10 that shows a delay of several minutes between the application of the stress and the detection of charge packets. On the other hand, it is difficult to reach a conclusion here because the progressive DC stress test involves, at each level of field, the effect of the charges accumulated during the previous steps, which is not the case in the charge profile measurement procedure. If a similar procedure (polarization/depolarization during 3600 s) is used to detect EL, the existence of transient luminescence (reported in § 3.2, with an example shown in Figure 14) which could have its own excitation process precludes any conclusion on the correlation between continuous EL excitation and charge packet formation. To discuss this point on a firm ground, we have performed charge profile measurements during the same progressive DC stress test as the one used to define the onset for continuous EL.

3.3.2.Charge profiles by using a progressive DC stress test

A progressive DC stress test has been carried out under the same conditions as for EL onset detection, using a gold-metallized sample of cable C for which the onset for continuous EL was ≈65 kV/mm. All space charge measurements were made simultaneously with the current in the external circuit [5,18]. The charge profiles have been measured continuously over each step. Almost no change was observed over the duration of the step and the charge profiles shown in figure 15 are those recorded at the end of the step just prior to increasing the applied field. It should be noted, however, that the simultaneously measured external current showed a transient response. Figure 15 shows the evolution of the charge profiles as a function of field. Up to 50 kV/mm, the profiles are dominated by homocharge at the anode extending deep into the sample. For these fields the transient current was dominant. At 60 to 65 kV/mm the negative homocharge starts to penetrate into the sample from the region of the cathode. At this field the external current started to approach a constant value during the step (i.e. it reaches a DC level). At higher fields, the negative charge penetration becomes more and more pronounced and an interface can be defined between positive and negative space charge approximately in the middle of the sample. There is no evidence of a charge packet. The saturation level of the external current follows a non-linear relationship with the applied field. Thus an applied field of 60-65 kV/mm marks the formation of a charge interface in the sample caused by penetration of the negative charge which is

related to the onset of a transport mechanism that allows the negative space charge region to advance. The change in transport mechanism, evidenced also by a change in current-field characteristics in the external current at 60-65kV/mm, allows us to correlate these experiments with the EL measurements for which the observation of continuous EL is associated with a similar modification of the I-E behaviour, see figure 4. These results clearly demonstrate that continuous EL excitation can be started without the mediation of charge packets, in situations where positive and negative charge fronts interact in the bulk. However, this does not preclude a specific EL pattern during charge packet propagation. This topic is addressed in the following section.

3.4. Electroluminescence during charge packet propagation

Electroluminescence and current have been recorded up to 48 hours at 120 kV/mm and 150 kV/mm, i.e. at field levels were charge packets were evidenced (see Figure 10). A XLPE sample of cable C was used for this experiment, the voltage being raised according to a progressive DC stress test. As for the experiment at 120 kV/mm, the details of the procedure is as follows:

-from 0 to 120 kV/mm: steps of 4.0 kV/mm with a 300 s of duration,

-at 120 kV/mm: EL and current are recorded in steps of 5s, for 48 hours,

-from 120 kV/mm to 0: steps of 7 kV/mm with 60 s in duration.

The experiment at 150 kV/mm was performed after overnight short-circuit of the sample. A similar procedure was used to target a field level of 150 kV/mm:

-from 0 to 150 kV/mm: steps of 6.0 kV/mm with a 300 s of duration,

-at 150 kV/mm: EL and current are recorded in steps of 5s, for 48 hours.

Current and electroluminescence are given vs. time in Figures 16a and 16b at 120 kV/mm and 150 kV/mm respectively. From the two sets of data, it appears clearly that oscillations are being detected in both current and EL, and that they are well correlated in time. Three different periods of time can be considered regarding the experiment at 120 kV/mm. For the whole time range, there is a constant level of EL that is significantly higher than the PM noise, which likely corresponds to a continuous EL excitation level. Up to about 20 h, one observed several current maxima of decreasing amplitudes, each of those being associated with a corresponding EL maximum. Then, from 21 h on, one observes a considerable level off of the EL, followed by a slow decrease. This process is correlated with a slight level off of the current, although its variation does not follow the EL variation as in the previous period of time. Turning to the experiments performed at 150 kV/mm, and if we exclude the transient EL observed during the first three hours, the same kinds of conclusion can be drawn; current oscillations match reasonably well the EL oscillations.

The order of magnitude of the current and EL oscillation frequency recorded in this work varies from 2 to 3 hours. In some situations, the EL is not reflected by the current variation, typical examples being the slow EL transient observed up to three hours for the 150 kV/mm experiment, and also the EL peak observed at about 21 h for the 120 kV/mm experiment. As for the current oscillations, they

have been clearly associated with charge packet propagation [**8, 18**]. In particular, it was noticed that they have the same period of oscillation, which depends on field and on investigated material. It has to be underlined that the maximum of the external current oscillation is associated with the collapse of the propagating packet at or near the opposite electrode [**18, 25**]. The time dependence of current and EL shown in Figure 16a (120 kV/mm) and 16b (150 kV/mm) can be compared with the 3D-charge profiles shown in Figure 10c (130 kV/mm) and 10d (150 kV/mm), although the latter have not been followed for so long times and have not been obtained on the same XLPE. At 130 kV/mm, Figure 10c shows that a negative packet is propagating towards the anode, followed by the launch of a positive packet. The time they take to reach the mid-gap can be taken as a rough evaluation of the frequency of the packets, that is about 3 h, which is well correlated with the frequency of 2 h determined from the EL and current oscillations at the same field (120 kV/mm in fact). The appearance of the first maximum in current is also well correlated with the transit time of the first negative packet, although the procedure used to apply the voltage was different. Results at 120 kV/mm are consistent, both regarding frequencies of charge packet, current, and EL oscillations. At 150 kV/mm, Figure 10d shows that the charge packet frequency is much shorter, of the order of 30 min. Comparison with Figure 16b shows that transient EL is detected during the first three hours, starting from a level of 3000 c/5 s and decreasing regularly to 55 c/5 s, without apparent amplitude modulation or relationship with the external current. The absence of current oscillations in the period of time where transient EL was detected could mean that charge packets were not produced. We think this peculiarity could be due to the previous charging of the sample during the experiment at 120 kV/mm, even though it was short-circuited overnight before being used for the experiment at 150kV/mm.

Although further investigation is needed to understand the transient emission, two main conclusions can be drawn. First, the propagation of charge packets has been associated with a specific luminescence pattern, thereby confirming that the excitation is due to charge recombination. Both current and EL oscillations are almost in phase in time, suggesting that recombination is occurring during the propagation of the packet. The time resolution, however, is not sufficient to determine if the recombination occurs throughout the body of the packet or at the rear as implied by the mechanism described in [21]. The maximum of the emission corresponds to the collapse of the charge packet at or near the opposite electrode, but this is also correlated with the launch of subsequent packet, thereby suggesting that recombination could also be operant in the vicinity of the injecting electrode (injected charges recombining heterocharges). Second, EL can be emitted in a more efficient way in situations where charge packets were not evidenced on the basis of the current measurements.

4. CONCLUSION

The objective of the paper was to cross-correlate information obtained from electroluminescence and charge distribution measurements in XLPE materials submitted to a DC field. The samples consisted

in 150 μm-thick peelings taken from the insulation of three reference cables that differed only by slight changes in the extrusion process. A thermal treatment was carried out before any test in order to expel most of the residues due to the cross-linking process. The experiments were not performed for the purpose of comparing the different materials, and the results show in fact a very similar behaviour in agreement with the identical formulation of the XLPE, although slight differences were noticed in quantitative values of some parameters (e.g., onset field for charge accumulation).

The main conclusion drawn from this study is that electroluminescence processes are associated with the presence of space charge and depend on its internal distribution. In particular, EL emission was never evidenced in a condition where space charge would not have been measurable with the typical sensitivity of the pulse electro-acoustic technique (0.1 $C.m^{-3}$).

Three other important points have to be noticed:

-(1) Fields of the order of ≈20 kV/mm (material dependent) constitutes a limit above which there is evidence of space charge accumulation. This space charge is able to trigger off energetic processes, leading to photon emission, upon fast modification of the applied voltage such as the one encountered during sample grounding. It gives a further support to the proposal that the above-mentioned field value constitutes a degradation threshold, owing to the inherent relationship between electroluminescence and ageing.

-(2) From ≈60/70 kV/mm on, the space charge acquires a dynamic character relative to the situation at lower field, with two noticeable effects: a continuous excitation of the EL and the formation of charge packets that propagate through the dielectric. The onset field for the two effects is in exact correlation with a change in the transport process as revealed by the analysis of the current-voltage characteristic. We have shown that the continuous excitation of the EL is due to recombination phenomena induced by the formation of positive and negative homocharge regions, which interact in the bulk of the sample, prior to the development of charge packet. Both EL and charge packet are ancillary to the formation of a bipolar charge distribution. Continuous excitation of EL by hot electrons in a unipolar scheme has to be ruled out in favor of an excitation by charge recombination in a bipolar scheme. We have shown that charge packets go along with oscillations in current and luminescence that are almost in phase in time. This is the expected behavior for either of the current models of charge packet formation and cannot be used to separate them as candidates for the charge packets observed here without a better time resolution. Consideration of EL together with the charge profile underlines the fact that the actual local charge density in the material might be much higher than the charge density derived from space charge detection techniques, owing to the fact that these techniques are only sensitive to the net charge.

-(3) The third point to be noted is the existence of transient excitation of the EL during voltage variation. Although we have not performed a detailed analysis on this point, it appears that peculiar excitation mechanism of the EL could be involved, such as injection induced luminescence with

mediation of hot carriers. More work is needed to understand the excitation mechanism of the EL on transient voltages.

Acknowledgements

This work was carried out under the ARTEMIS program EU contract Number BRPR-CT98-0724. The authors thank the ARTEMIS publications committee and the EU for permission to publish.

REFERENCES

1. Hozumi N, Takeda T, Suzuki H and Okamoto T 1998 Space charge behavior in XLPE cable insulation under 0.2-1.2 MV/cm dc field *IEEE Trans. DEI* **5** 82-90.
2. Li Y and Takada T 1992 Experimental observation of charge transport and injection in XLPE at polarity reversal *J. Phys. D : Appl. Phys*.**25** 704-716.
3. Bambery K R and Fleming R J 1998 Space charge accumulation in two power cable grades of XLPE *IEEE Trans. DEI* **5** 103-109.
4. Ho Y F F, Chen G, Davies A E, Hampton R N, Hobdell S, Swingler S G and Sutton S 2000 Space charge measurements in XLPE insulation under 50 Hz AC electric stress *Proc. Eight International Conference on Dielectric Materials, Measurements and Applications* (Edinburgh, UK) pp. 68-73.
5. Fothergill J C, Dissado L A, Alison J and See A 2000 Advanced pulsed electro-acoustic system for space charge measurement *Proc. Eight International Conference on Dielectric Materials, Measurements and Applications* (Edinburgh, UK) pp. 352-356.
6. Montanari G C, Mazzanti G, Boni E and De Roberties G 2000 Investigating AC space charge accumulation in polymers by PEA measurements *Proc. Conference on Electrical Insulation and Dielectric Phenomena* (Victoria, Canada) pp. 113-116.
7. Bert C, Heninion C, Lewiner, Alquié J C, Hampton N, Freestone J and Verne S 1995 Measurement of space charge distribution under 50 Hz A.C. stress *Proc. Fourth International Conference on Insulated Power Cables* (Versailles, France) pp. 195-199.
8. Hozumi N, Suzuki H, Okamoto, Watanabe T K and Watanabe A 1994 Direct observation of time-dependent space charge profiles in XLPE cable under high electric fields *1994 IEEE Trans. DEI* **1** 1068-1076.
9. Fukuma M, Nagao M, Kosaki M and Kohno Y 1999 Measurements of conduction current and electric field distribution up to electrical breakdown in LDPE film *Proc. Conference on Electrical Insulation and Dielectric Phenomena* (Austin, USA) pp 144-147.
10. Laurent C 1998 Optical pre-breakdown warnings in insulating polymers *Proc. International Conference on Conduction and Breakdown in Solid Dielectrics* (Västeras, Sweden), pp. 1-12.
11. Zeller H R 1991 Non insulating properties of insulating *materials Proc. Conference on Electrical Insulation and Dielectric Phenomena* (Knoxville, USA), pp 19-47.
12. Sanche L 1993 Electronic aging and related electron interactions in thin-film dielectrics 1993 *IEEE Trans. on EI* **28** 789-819.
13. Zeller H R, Pfluger P and Bernasconi J 1984 High-mobility states and dielectric breakdown in polymeric dielectrics *IEEE Trans. DEI* **19** 200-204.
14. Kitani I, Hirano T and Arii K 1987 Very faint light emission in low-density polyethylene films under DC field *Jpn. J. Appl. Phys*.**26** 639-640.

15. Montanari G C 2000 The electrical degradation threshold of polyethylene investigated by space charge and conduction current measurements *IEEE Trans. DEI* **7** 309-315.
16. Dissado L, Mazzanti G and Montanari G C 1997 The role of trapped space charges in the electrical aging of insulating materials *IEEE Trans. DEI* **4** 496-506.
17. Augé J L, Fabiani D, Laurent C and Montanari G C 2000 Investigating DC thresholds in polyethylene by space-charge, current and electroluminescence measurements *IEEE Trans. DEI* **7** 797-803.
18. Alison J M 1998 A high field pulsed electro-acoustic apparatus for space charge and external circuit current measurement within solid insulators *Meas. Sci. Technol*. **9** 1737-1749.
19. Kon H, Suzuoki Y, Mizutani T, Ieda M and Yoshifuji N 1996 Packet-like space charges and conduction current in polyethylene cable insulation *IEEE Trans. DEI* **3** 380-391.
20. Fothergill J C 2000 Space charge in dielectrics: old theories and new measurements *Proc. Eight International Conference on Dielectric Materials, Measurements and Applications* (Edinburgh, UK), pp. 1-5.
21. Kaneko K, Mizutani T and Suzuoki Y 1999 Computer simulation on formation of space charge packets in XLPE films *IEEE Trans. DEI* **6** 152-158.
22. Dissado L, Fothergill J, See A, Stevens G, Markey L, Laurent C, Teyssedre G, Nilsson U H, Platbrood G and Montanari G C 2000 Characterizing high-voltage XLPE cables through electrical and microstructural measurements performed on cable peelings: the effect of surface roughness and thermal treatment *Proc.Conference on Electrical Insulation and Dielectric Phenomena* (Victoria, Canada), pp. 136-140.
23. Mary D, Albertini M and Laurent C 1997 Understanding optical emissions from electrically stressed insulating polymers : electroluminescence in poly(ethylene terephthalate) and poly(ethylene 2, 6-naphthalate) films *J. Phys. D.: Appl. Phys*.**30** 171-184.
23. Augé J L, Teyssedre G, Laurent C, Ditchi T and Holé S 2000 Combined electroluminescence and charge profile measurements in poly (etylene-2, 6-naphthalate) under DC field *J.Phys.D:Appl.Phys*.**33** 3129-3138.
24. Suzuoki Y, Kon H, Kaneko K, Mizutani T and Itaya T 1998 Packet-like space charge behaviour in insulating polymers, in *Space Charge in Solid Dielectrics,* The Dielectrics Society Ed., UK.

FIGURE CAPTIONS

Table 1: Values of the onset field for continuous electroluminescence excitation in the three kinds of XLPE peelings

Figure 1: Schematic of the electroluminescence excitation mechanisms in a dielectric submitted to a uniform dc field. The most probable regions of emission are indicated in grey. Solid lines indicate absolute values of the field.

a-Hot carrier-induced luminescence in a space charge free dielectric submitted to pre-breakdown field

b-Hot carrier-induced luminescence in the field-enhanced region of a dielectric with unipolar injected space charge

c-Recombination-induced luminescence in a dielectric with bipolar injected space charge.

Figure 2: Charge packet in XLPE interpreted as a propagating ionisation front and associated recombination-induced luminescence.

The horizontal axis is distance through the material. The two curves correspond to space charge density (the positive "hump" is the charge packet) and the field (bottom curve). Cathode on the left, anode on the right. Taken from [20].

Figure 3: EL under a progressive DC stress test (XLPE B)

a-During voltage cycle up to 120 (1) and 150 (2) kV/mm

b-As a function of time for different fields

Figure 4: Current and EL versus field for the two voltage cycles (XLPE B)

Current values were taken after 300 s of polarization. They are not representative of the permanent conduction.

Figure 5: Current-field characteristic for XLPE B.

Current values were taken after 24 hours of polarization at each step. The characteristic can therefore be considered as a good approach of the transport process.

Figure 6: Current and EL versus field for XLPE A

Current values were taken after 300 s of polarization. They are not representative of the permanent conduction.

Figure 7: Charge profiles for field lower than the onset for continuous EL excitation.

t_p = poling time, t_0 = depolarisation time.

a-Time dependence of the charge profiles during polarization and in volt off, for different fields

b-Field dependence of the charge profiles taken at the end of the polarization period

(volt-on measurements at 10000 s)

Figure 8: EL transients observed during voltage application and sample grounding.

a-During voltage application at 40 kV/mm (sampling time is 1 s)

b-During sample grounding at 50 kV/mm (sampling time is 1 ms)

Figure 9: Quantification of stored charge and transient EL at short-circuit (XLPE A)

a-Stored charge versus poling field obtained from space charge measurements

b-Integrated EL at the short-circuit versus poling field. Counts due to background noise of the PM have been substracted from the integrated signal.

Figure 10: Spatio-temporal evolution of the net charge during polarization and depolarization at different fields (XLPE B). Each representation has three dimensions: thickness, time and charge. Thickness is the Y axis (cathode and anode are indicated), time is the X axis (non linear scale), and the 3rd dimension is charge, represented by a colour scale. There are 20 different colours that represent 20 levels of charge in a decimal scale; a maximum value of charge (x) is chosen and divided into the 20 levels for each pattern. x=20 C.m^{-3} for Fig.10a and 10b; x=40 C.m^{-3} for Fig. 10c and 10d. All the values exceeding the maximum level, positive or negative, are associated with the white. This happens at the electrodes where the applied voltage leads to high values of capacitive charges.

Figure 11: Charge profiles in volt-off condition at time 10010 s (t_0 = 10s), for different fields (XLPE B). Cathode on the left, anode on the right.

Figure 12: Charge profiles in volt-on condition vs time, for different fields (XLPE B)

a-Charge profiles relevant to poling field of 80 kV/mm, (1)-at time 200 s, (2)-at time 1100 s

b-Charge profiles relevant to poling field of 130 kV/mm, (1)-at time 700 s, (2)-at time 10000 s

c-Field distribution relevant to the charge profiles shown in b

Figure 13: Charge and field profiles during launching, propagation, and collapse of the first positive packet detected at 150 kV/mm (XLPE B)

a-Upon launching (t=450s), b-upon propagation (t=2100s), c-upon collapse (t=3000s)

Figure 14: Transient EL observed at voltage application in a stepped voltage experiment for a field of 80 kV/mm.

Figure 15: Charge profiles at different fields for a progressive DC stress test (XLPE C)

Anode on the left, cathode on the right. Profiles are shown at 60kV/mm, 72 kV/mm, 80 kV/mm, 88 kV/mm, 96 kV/mm, 104 kV/mm, 112 kV/mm and 120kV/mm

Figure 16 : EL and current under long term DC stress test (XLPE C)

(a)-120 kV/mm, (b)-150 kV/mm

Arrows indicate current and electroluminescence oscillations.

Table 1: Values of the onset field for continuous electroluminescence excitation for the three kinds of XLPE peelings

Reference of XLPE peeling	Onset for continuous EL detection (kV/mm)
A	60-70
B	60-65
C	60-70

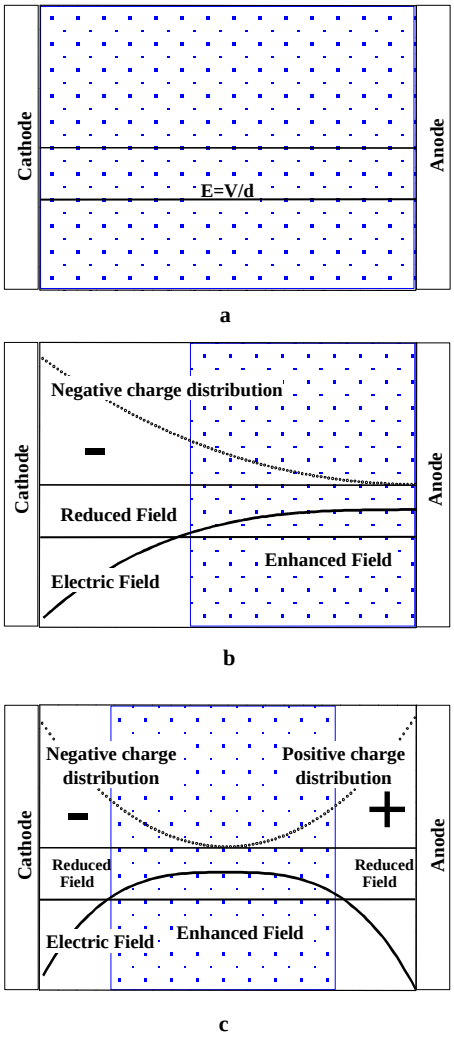

Figure 1: Schematic of the electroluminescence excitation mechanisms in a dielectric submitted to a uniform DC field. The most probable regions of emission are indicated in grey. Solid lines indicate absolute values of the field.

a-Hot carrier-induced luminescence in a space charge free dielectric submitted to pre-breakdown field

b-Hot carrier-induced luminescence in the field-enhanced region of a dielectric with unipolar injected space charge

c-Recombination-induced luminescence in a dielectric with bipolar injected space charge.

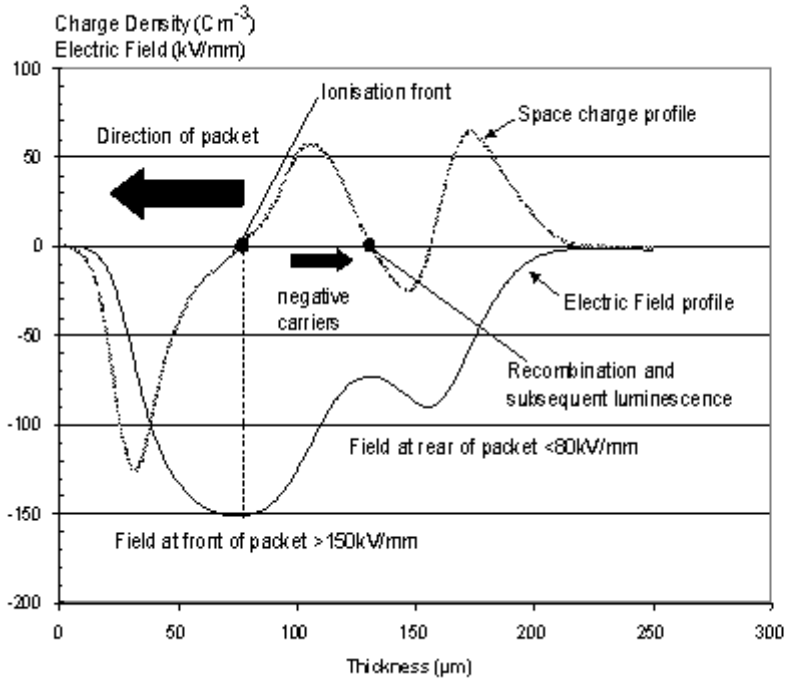

Figure 2: Charge packet in XLPE interpreted as a propagating ionisation front and associated recombination-induced luminescence.

The horizontal axis is distance through the material. The two curves correspond to space charge density (the positive "hump" is the charge packet) and the field (bottom curve). Cathode on the left, anode on the right. Taken from [20].

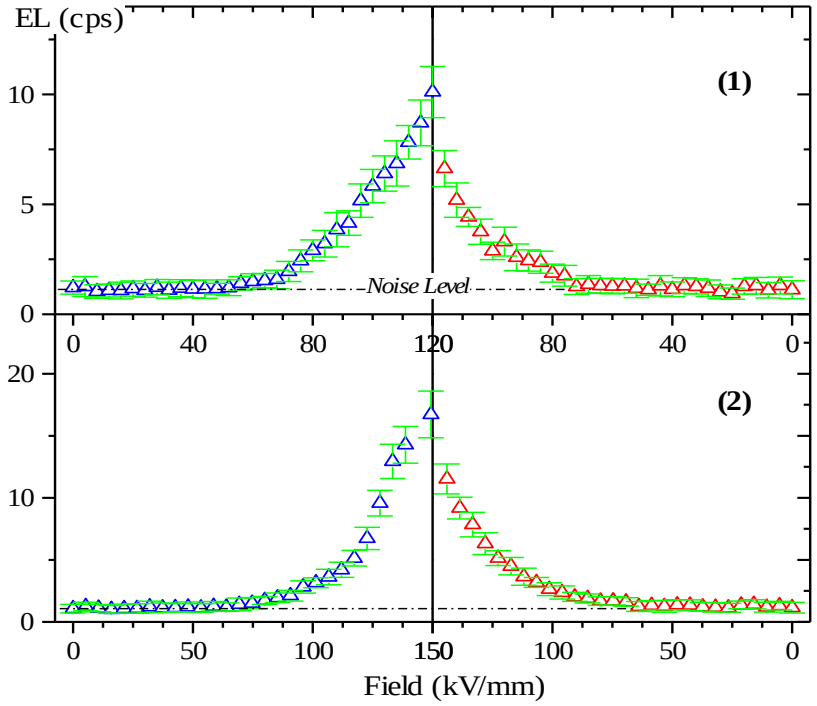

a-During voltage cycle up to 120 (1) and 150 (2) kV/mm

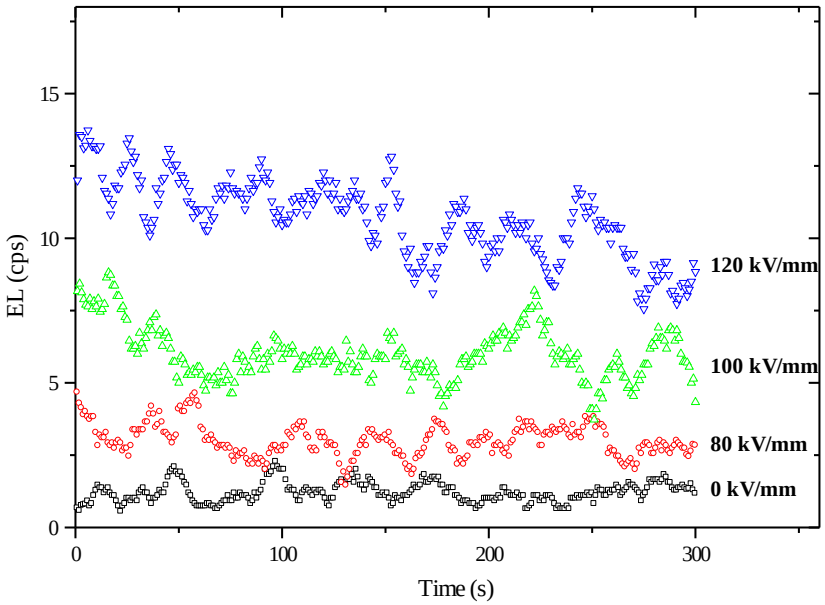

b- As a function of time for different fields.

Figure 3: EL under a progressive DC stress test (XLPE B)

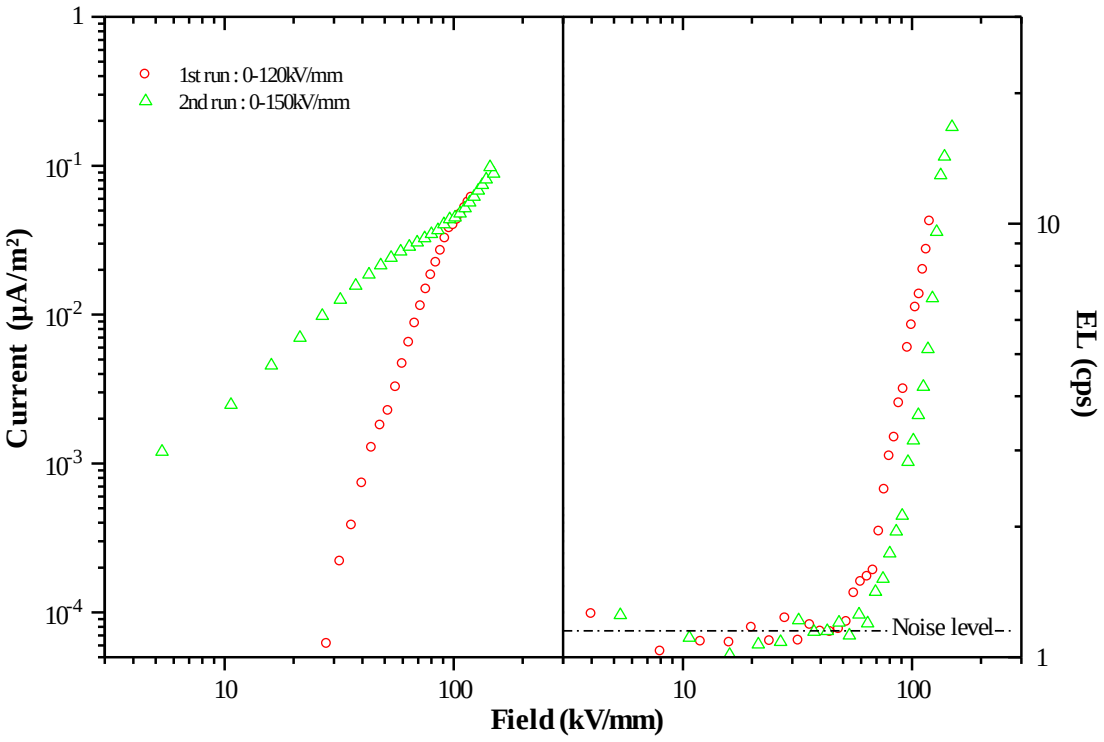

Figure 4 : Current and EL versus field for cycles run as indicated (XLPE B). Current was measured after 300s of polarization. It is not representative of the permanent conduction.

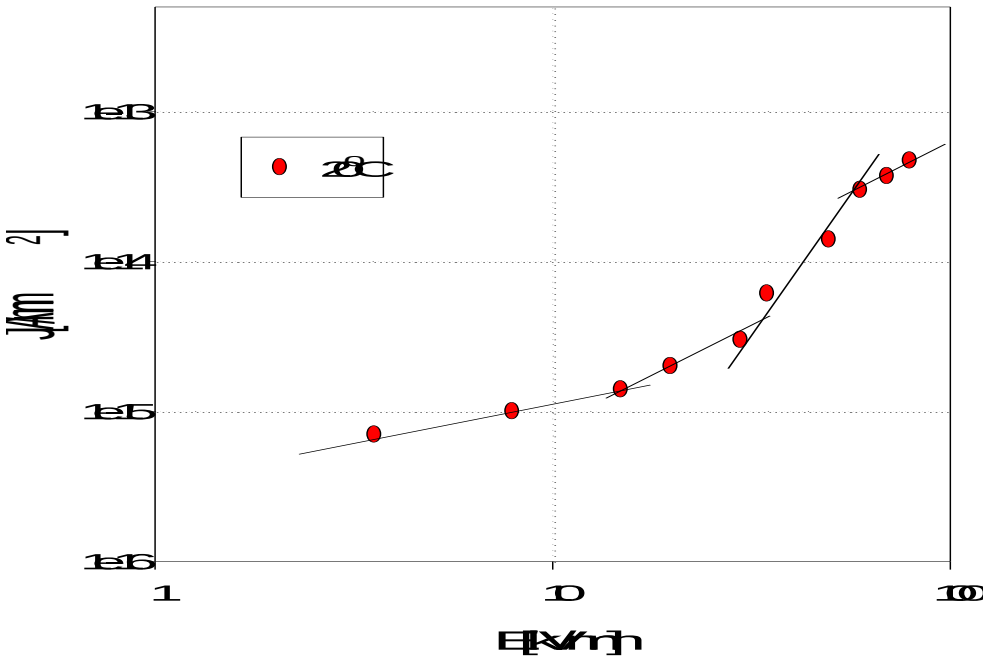

Figure 5: Current-field characteristic for XLPE B.

Current values were taken after 24 hours of polarization at each step. The characteristic can therefore be considered as a good approach of the transport process.

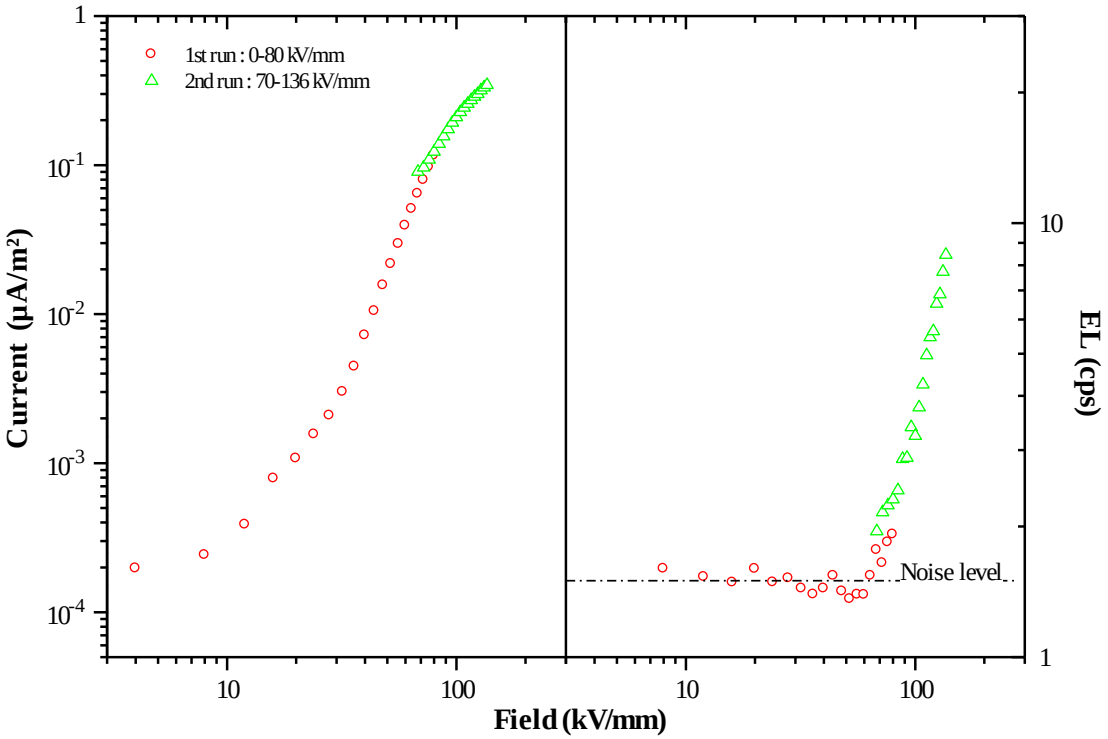

Figure 6 : Current and EL versus field for cycles run as indicated (XLPE A). Current was measured after 300s of polarization. It is not representative of the permanent conduction.

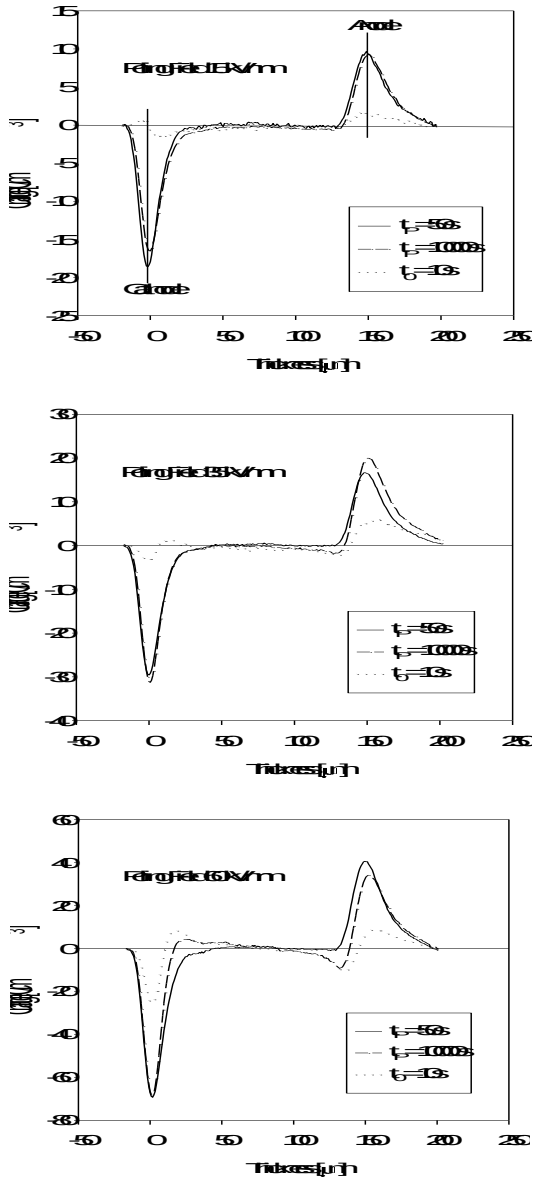

a-Time dependence of the charge profiles during polarization and in volt off, for different fields

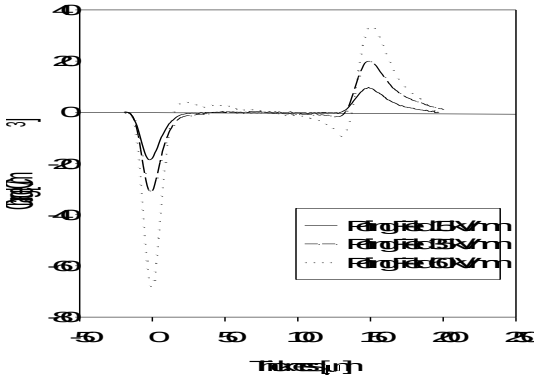

b-Field dependence of the charge profiles taken at the end of the polarization period

(volt-on measurements at 10000 s)

Figure 7: Charge profiles for field lower than the onset for continuous EL excitation.

t_p = poling time, t_0 = depolarisation time.

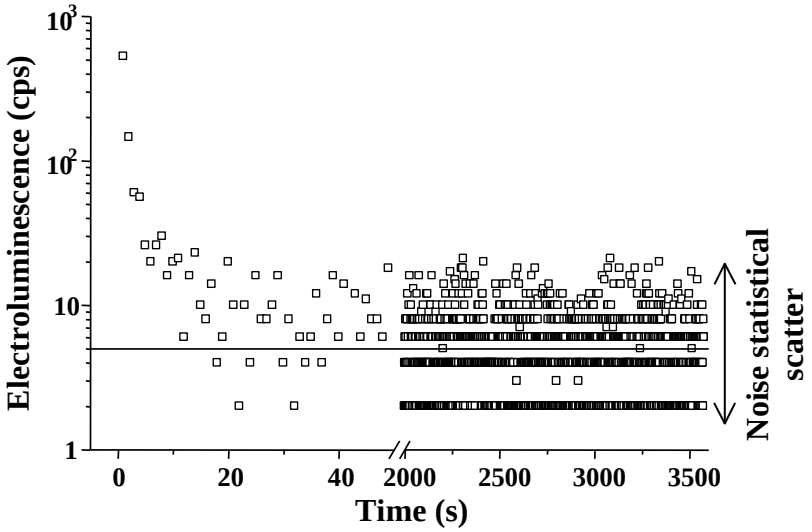

a-During voltage application at 40 kV/mm (sampling time is 1 s)

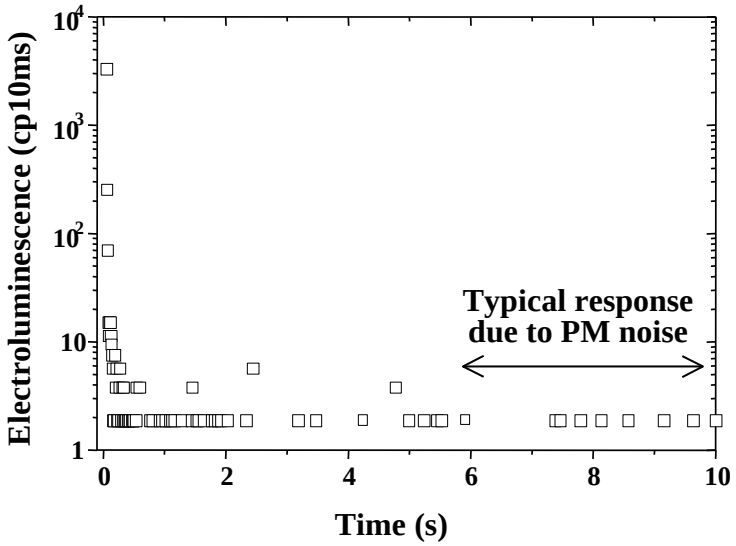

b-During sample grounding at 50 kV/mm (sampling time is 10 ms)

Figure 8: EL transients observed during voltage application and sample grounding

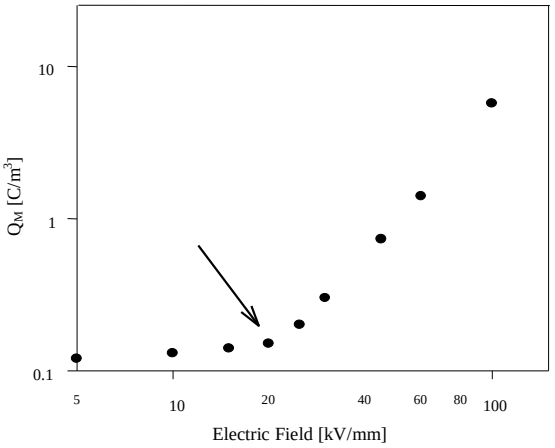

a-Stored charge versus poling field obtained from space charge measurements

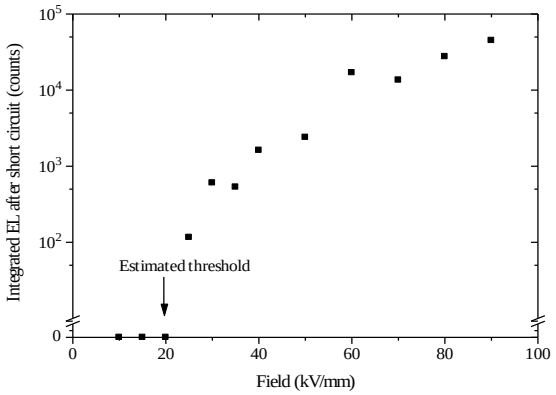

b-Integrated EL at the short-circuit versus poling field. Counts due to background noise of the PM have been substracted from the integrated signal.

Figure 9: Quantification of stored charge and transient EL at short-circuit (XLPE A)

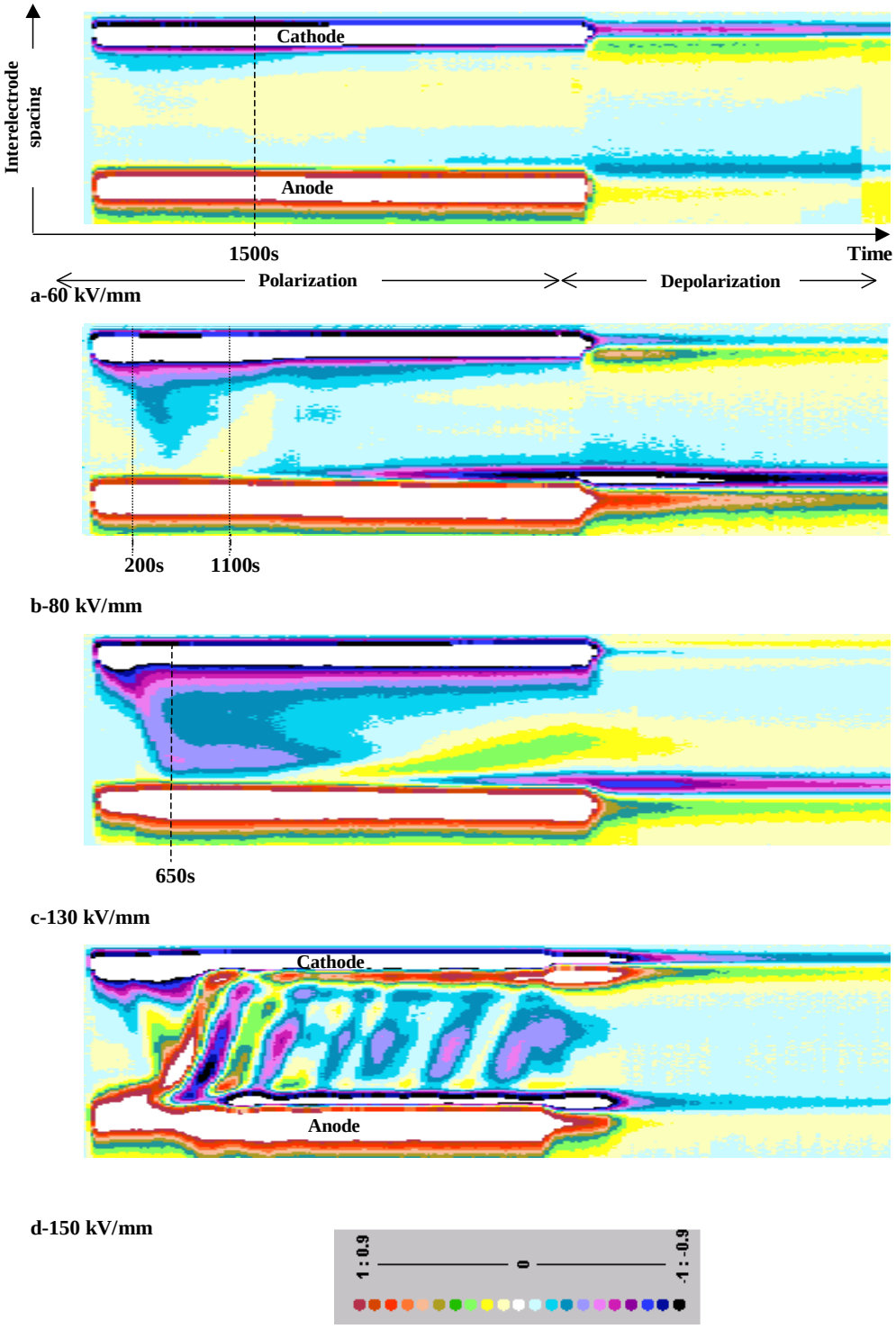

Figure 10: Spatio-temporal evolution of the net charge during polarization and depolarization at different fields in XLPE B. Each representation has three dimensions: thickness, time and charge. Thickness is the Y axis (cathode and anode are indicated), time is the X axis (non linear scale), and the 3rd dimension is charge, represented by a colour scale. There are 20 different colours that represent 20 levels of charge in a decimal scale; a maximum value of charge (x) is chosen and divided into the 20 levels for each pattern. x=20 $C.m^{-3}$ for Fig.10a and 10b; x=40 $C.m^{-3}$ for Fig. 10c and 10d. All the values exceeding the maximum level, positive or negative, are associated with the white. This happens at the electrodes where the applied voltage leads to high values of capacitive charges.

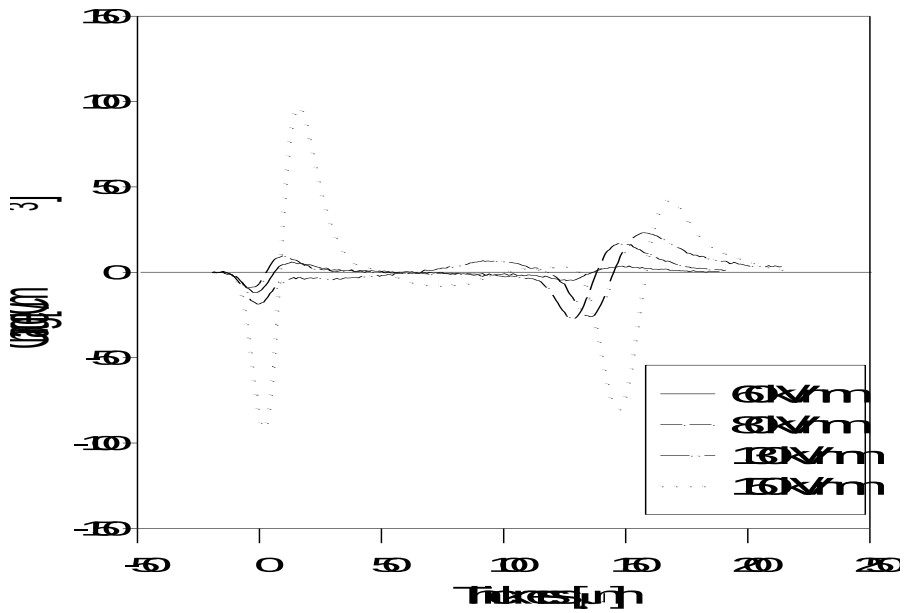

Figure 11: Charge profiles in volt-off condition at t_0 = 10s, for different fields (XLPE B)

(cathode on the left, anode on the right)

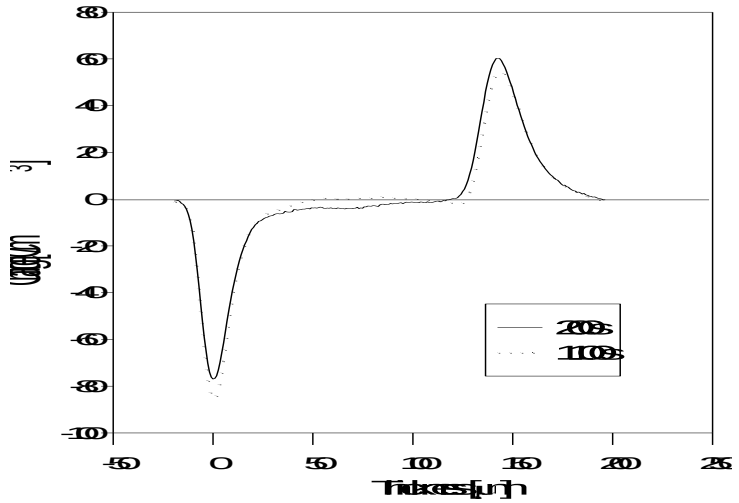

a-Charge profiles relevant to poling field of 80 kV/mm

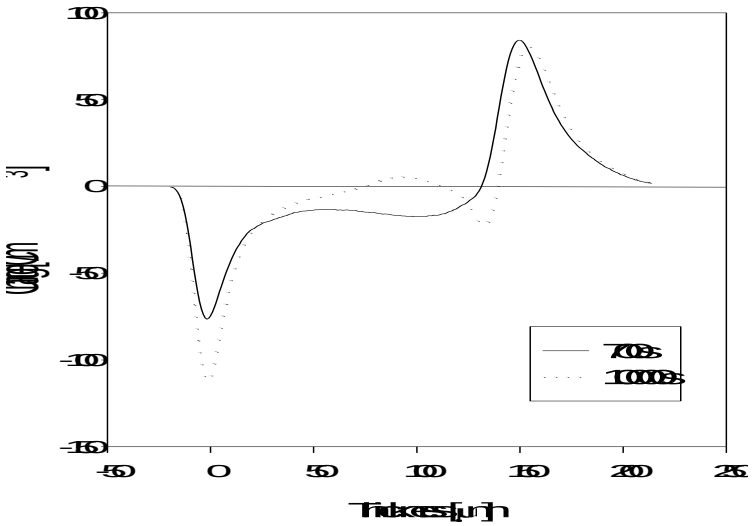

b-Charge profiles relevant to poling field of 130 kV/mm

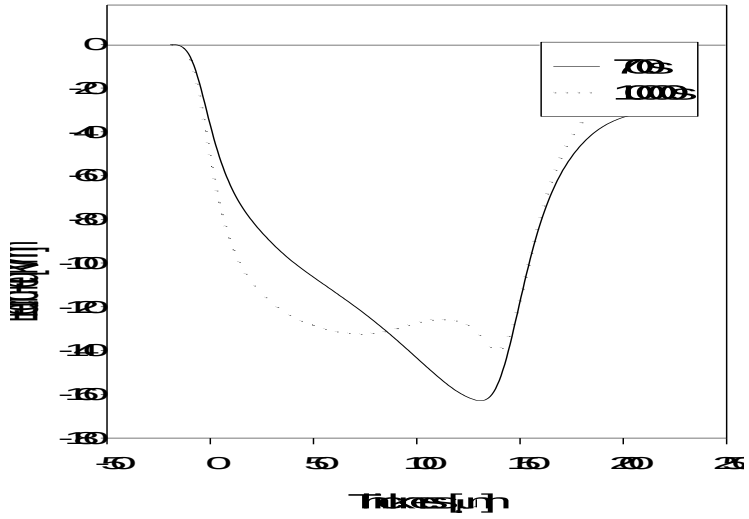

c-Field distribution relevant to the charge profiles shown in **b**

Figure 12: Charge and field profiles in volt-on condition for different fields (XLPE B)

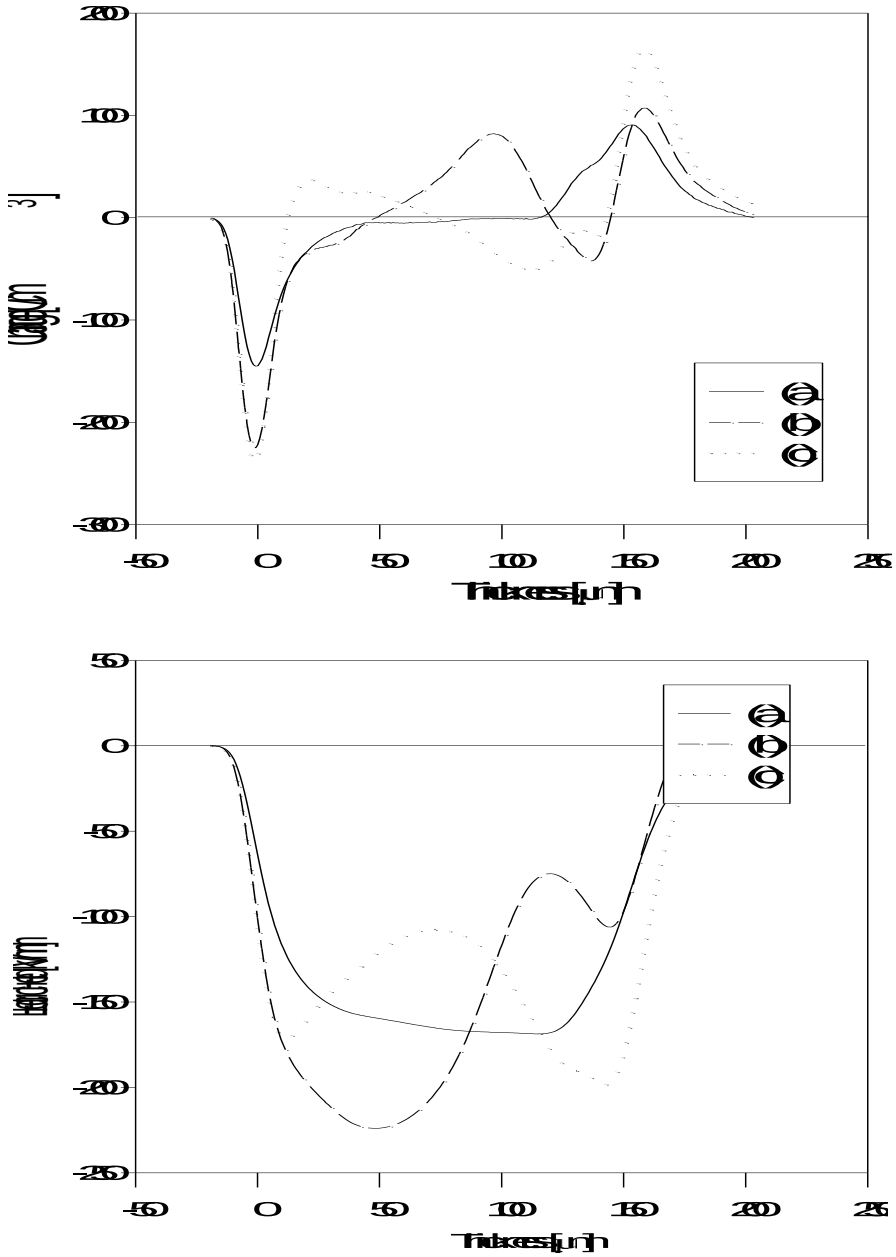

Figure 13: Charge and field profiles during launching, propagation, and collapse of the first positive packet detected at 150 kV/mm (XLPE B)

a-Upon launching (t=450s), b-upon propagation (t=2100s), c-upon collapse (t=3000s)

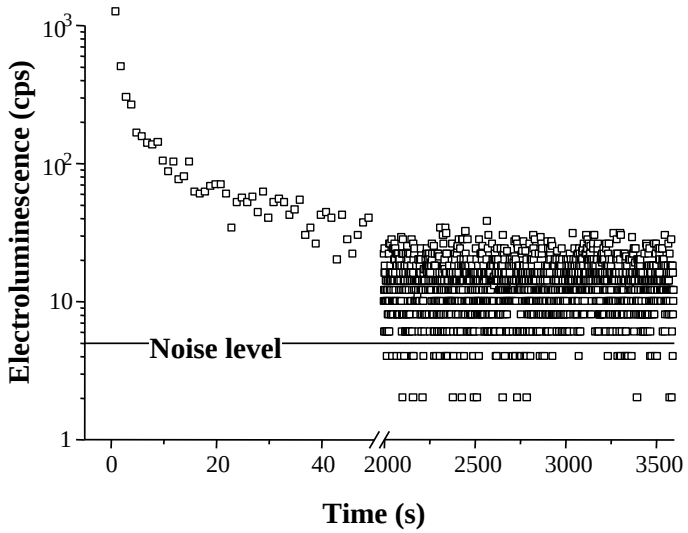

Figure 14: Transient EL observed at voltage application in a stepped voltage experiment for a field of 80 kV/mm

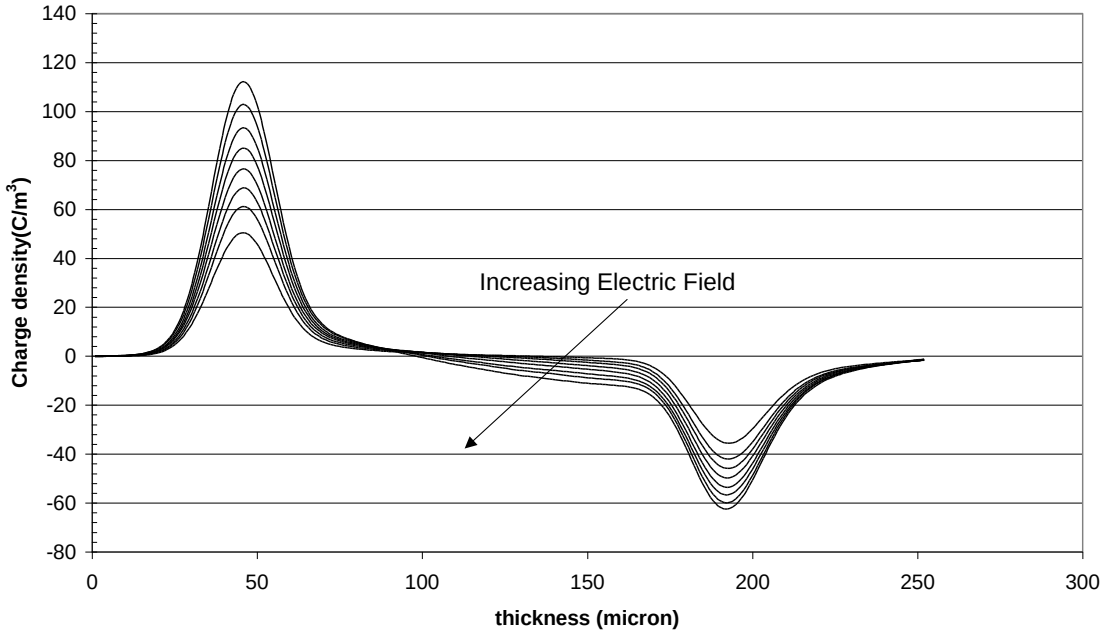

Figure 15: Charge profiles at different fields for a progressive DC stress test (Cable C)

Cathode on the right, anode on the left.

Profiles are shown at 60kV/mm, 72 kV/mm, 80 kV/mm, 88 kV/mm, 96 kV/mm, 104 kV/mm, 112 kV/mm and 120kV/mm

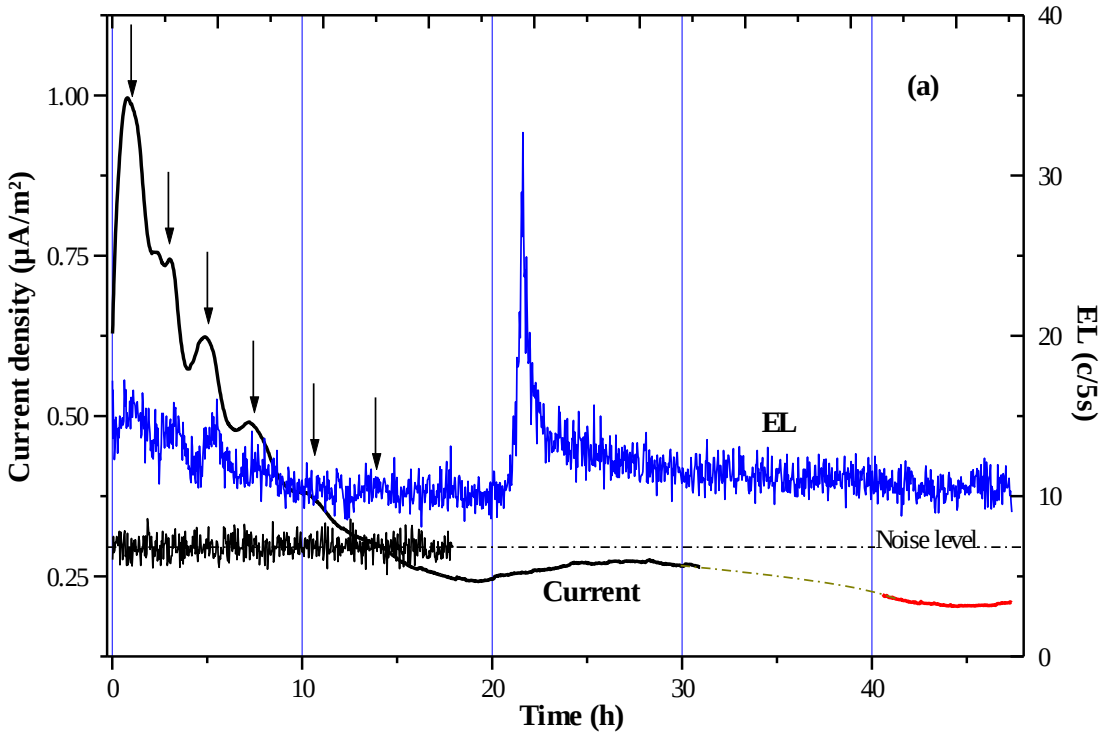

a- At 120 kV/mm.

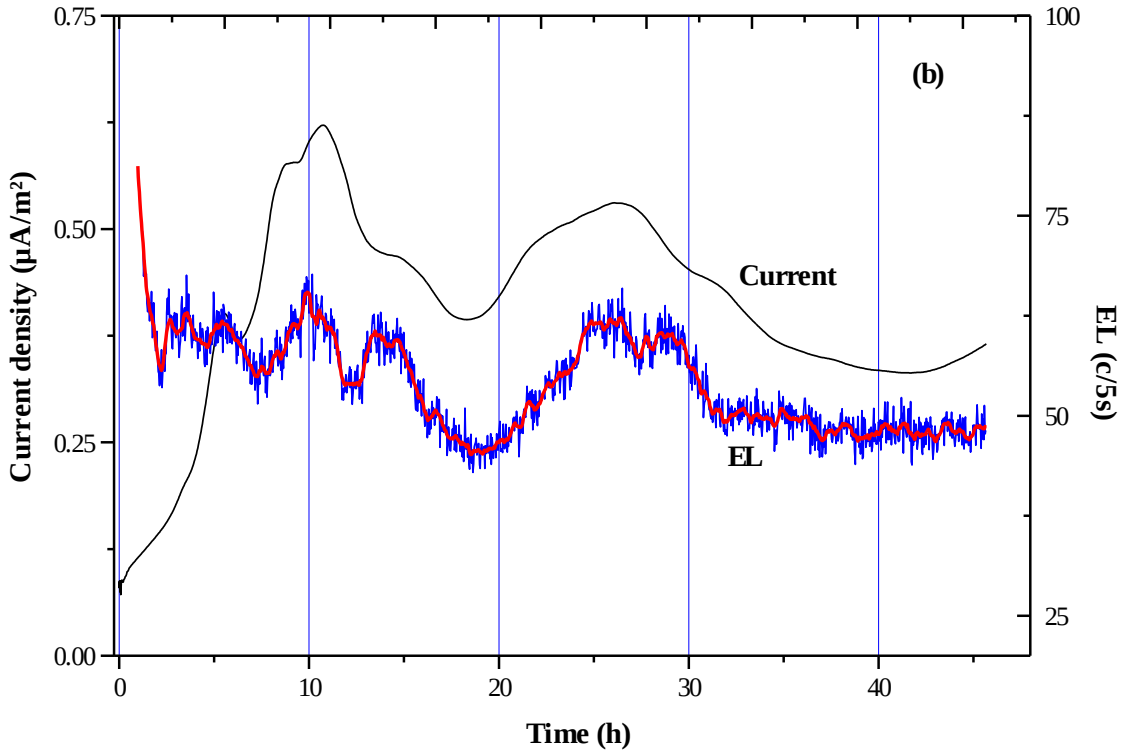

b- At 150 kV/mm.

Figure 16 : EL and Current under long term DC stress test (XLPE C)

Arrows indicate current and electroluminescence oscillations